REVISTAMATÉRIA
V.29 N.3
ISSN 1517-7076 articles e20240303, 2024

Assessment of axial load carrying capacity of fully encased composite columns: comparative study with different codes

Saravanan Muthuchamy Maruthai[1], Sasikumar Palanisami[2]

[1]Vivekanandha College of Technology for Women, Department of Civil Engineering. 637205, Namakkal, Tamil Nadu, India.
[2]Kumaraguru College of Technology, Department of Civil Engineering. 641049, Coimbatore, Tamil Nadu, India.
e-mail: saromms@gmail.com, sasiserene@gmail.com

ABSTRACT

Currently, fully encased composite columns (FECCs) and high-strength concrete (HSC) are widely used in the construction industry to build durable structures. Specifically, HSC is primarily employed in high-rise buildings, highway bridges, and tunnels. This study examined eight FECC specimens with 200 mm × 250 mm × 1000 mm dimensions. Four FEC columns were considered control specimens, while the remaining four were cast with the optimum content of 0.60% Steel Fibre (SF). These specimens were fabricated with two different lateral reinforcement spacing: 100 mm and 80 mm. All specimens were tested under axial loading using a 500 T capacity frame. The main objective of this study was to evaluate the axial load-carrying capacity, axial load-deformation behaviour, ductility, stiffness, energy absorption capacity, and mode of failure of all FECC specimens. Adding 0.6% steel fibre and reduced lateral reinforcement spacing enhanced the specimens axial load-carrying capacity, ductility, and energy absorption capacity. The steel fibre was crucial in preventing concrete cover spalling and cracks on the specimens. Experimental test results for the FECC specimens were compared to various codes, including IS: 456 – 2000, JGJ 138-2016, and EN 1994-1-1. The present results were compared to previously published data and evaluated using the same codes. According to the experimental and analytical findings, the prediction results from JGJ 138-2016 and EN 1994-1-1 were highly correlated with the experimental results. EN 1994-1-1 is recommended for developing two proposed methods, which were also compared to the experimental test results. These proposed methods demonstrated good agreement with the experimental outcomes, with mean values of 1.08 and 1.06, standard deviations of 0.04, and coefficients of variation of 3.54% and 3.53% for proposed methods 1 and 2, respectively.

Keywords: Fully encased composite columns; High strength concrete; Peak ductility; Energy absorption capacity; Steel fibre.

1. INTRODUCTION

The FECC is widely used in the construction industry compared to the conventional Reinforced Concrete (RC) columns. The FECC had superior performances, such as resistance to shear cracks, resistance to buckling, high load-carrying capacity, and ductility [1]. Regarding fire resistance, Fiber-Encased Composite Columns (FECC) outperformed traditional reinforced concrete. This superiority arises from the steel section fully enveloping the concrete, providing enhanced protection against fire damage. Several studies have investigated FECC made with high-strength concrete under various loading conditions such as axial [2–9], uniaxial [10], eccentric [11, 12] and cyclic load [13]. Theoretical research examined by ELLOBODY and YOUNG [14] delved into the behaviour of axially loaded encased steel composite columns with concrete cylinder strengths ranging from 30 MPa to 100 MPa. These studies examined the experimental and analytical investigation of the FECC. The FECC specimens are made with high-strength concrete, which reduces the specimens' cross-section and increases the ductility and durability of the FECC [15–20]. Limited studies have investigated the various loading conditions, including axial load and combined axial load and bending moments. The FECC specimens are examined in different types: fully-encased composite columns, Partially-Encased Composite Columns (PECC) and Concrete-Filled Tubes (CFT) [21–23]. Additionally, the FECC specimens have superior performance and improved load-carrying capacity, ductility, corrosion resistance, fire resistance, stiffness, and seismic resistance compared to conventional RC columns [24–26].

Corresponding Author: Saravanan Muthuchamy Maruthai. Received on 25/05/2024 Accepted on 10/06/2024

DOI: https://doi.org/10.1590/1517-7076-RMAT-2024-0303

CHANG *et al.* [27] investigated how various factors affect the ultimate compressive strength of these double-skin tubular columns. The study compared experimental results with design approaches from three codes: GB50936 (2014), AISC (2010), and EC4 (2004). GB50936 (2014) yielded the best outcomes; AISC (2010) followed GB50936 in performance; and EC4 (2004) showed slightly lower performance. Interestingly, the type of in-filled concrete and interior tube material had no significant impact on sample performance at elevated temperatures. This research provides valuable insights into the field of structural engineering, especially in the context of composite columns. Combining steel, UPVC, and concrete offers promising possibilities for future construction practices. Several variables significantly impact the capacity of encased column sections. These variables include the height of the column, dimensions of the concrete encasement, area of the steel reinforcement, area of the steel core, strength of the concrete encasement, strength of the steel core, and strength of the steel reinforcement bars. According to the American Institute of Steel Construction (AISC) LRFD 2005 code, there are specific criteria that any column section must meet to be covered by this code. One critical limitation is the steel core area (A_s) ratio to the gross section area (A_g). The code specifies that A_s/A_g should not be less than 1.0%. Consequently, composite column sections with A_s/A_g values below 1.0% are designed as standard reinforced concrete columns, with the steel core serving as concentrated steel reinforcement. These columns then adhere to the terms and clauses outlined in the ACI code [28]. Concrete-encased composite structures combine concrete and structural steel (of various shapes) to provide load-carrying capacity for both axial and eccentric loads. The integral interaction between concrete and steel enhances ductility, stiffness, and cost-effectiveness. These structures are famous in high-rise buildings due to their seismic performance and space efficiency [29].

The primary objective of this study is to investigate fully encased concrete core (FECC) specimens. These specimens are examined for axial load-carrying capacity, axial load-deformation behaviour, ductility, stiffness, energy absorption capacity, and failure mode under axial loading conditions. The experimental results are then compared to various design codes, including IS: 456 – 2000 [30], JGJ 138-2016 [31], and EN 1994-1-1 [32]. The predicted results using JGJ 138-2016 and EN 1994-1-1 strongly correlate with the experimental findings. These codes serve as the foundation for developing two proposed methods that offer improved accuracy in predicting the experimental behaviour of FECC specimens. The flow of research methodology is depicted in Figure 1.

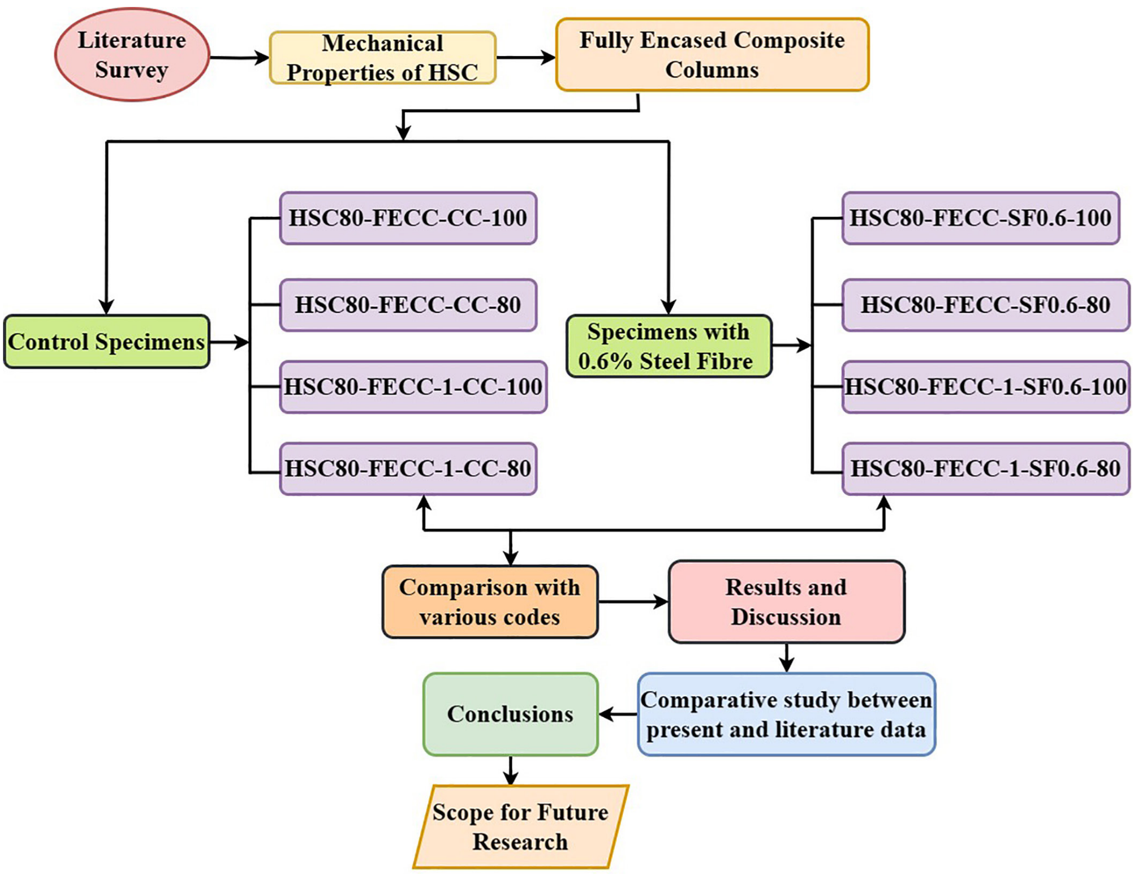

Figure 1: Research methodology of this research.

2. EXPERIMENTAL STUDY

2.1. Details of the materials

This study cast the FECCs with M75 HSC, High Yield Strength Deformed (HYSD) f_{yr} 500 rebar, and ISMB 100. Based on the experimental study, the optimum content of 0.6% SF was found. Beyond the optimum mix, the bond between the cement paste and aggregates is reduced, resulting in reduced strength. Hooked steel fibres with dimensions of a diameter of 0.75 mm, a length of 60 mm, and an aspect ratio of 80 were used. Two types of HSC mix were used, and their mechanical properties are reported in Table 1. The 12 mm rebar used in the primary reinforcement was tested under the Universal Testing Machine (UTM) capacity of 400 kN. Similarly, the steel section is tested under the loading frame capacity of 100 T. The mechanical properties of the steel section and rebar, including stress, strain, and modulus of elasticity, are evaluated. The stress-strain curve of the steel bar and steel section is shown in Figure 2.

2.2. Fabrication of specimens

Four groups were developed, and each group contains two specimens with dimensions of 200 mm × 250 mm × 1000 mm, as indicated in Table 2. All FECC specimens (including HSC80-FECC-CC-100, HSC80-FECC-SF0.6-100, HSC80-FECC-CC-80, HSC80-FECC-SF0.6-80, HSC80-FECC-1-CC-100, HSC80-FECC-1-SF0.6-100, HSC80-FECC-1-CC-80, and HSC80-FECC-1-SF0.6-80) are made with high-strength concrete. The first and second group specimens (HSC80-FECC-CC-100, HSC80-FECC-SF0.6-100, HSC80-FECC-CC-80, and HSC80-FECC-SF0.6-80) are cast with four numbers of HYSD rebar (each with a 12 mm diameter). Similarly, the third and fourth group specimens (HSC80-FECC-1-CC-100, HSC80-FECC-1-SF0.6-100, HSC80-FECC-1-CC-80, and HSC80-FECC-1-SF0.6-80) were cast with six numbers of HYSD 12 mm rebar. HYSD 6 mm diameter lateral reinforcements were used and provided at 100 mm spacing for the first two groups (HSC80-FECC-CC-100, HSC80-FECC-SF0.6-100, HSC80-FECC-CC-100 & HSC80-FECC-SF0.6-100) and 80 mm spacing for the latter two groups (HSC80-FECC-CC-80, HSC80-FECC-SF0.6-80, HSC80-FECC-CC-80 &

Table 1: Physical properties of high-strength concrete, steel section and reinforcement rebar.

PROPERTIES	CONCRETE	STEEL SECTION	STEEL REINFORCEMENT
Cube compressive strength (MPa)			
Control sample	79.63	–	–
Optimum simple (SF-0.6%)	86.42	–	–
Stress (MPa)	–	246.72	486.42
Strain	0.003	0.0021	0.002
Poisson ratio	0.3	0.28	0.29
Young's Modulus (GPa)	39.2	202	201

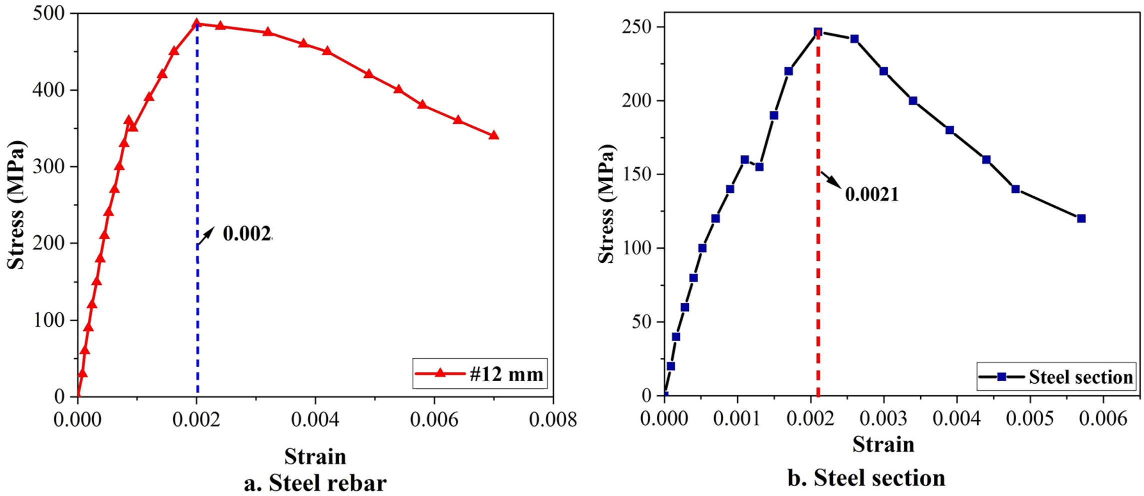

Figure 2: Stress-strain curve for steel rebar and section.

Table 2: Comparative study between experimental and analytical results.

SPECIMEN ID	SPECIMEN DIMENSION (mm)			STEEL SECTION (mm)				REINFORCEMENT DETAILS (mm)	
	BREADTH	DEPTH	LENGTH	BREADTH	DEPTH	T_W	T_F	MAIN REBAR	TIE REBAR
HSC80-FECC-CC-100	200	250	1000	50	100	7	4.2	4-#12 mm	#6 mm @ 100 mm c/c
HSC80-FECC-SF0.6-100	200	250	1000	50	100	7	4.2	4-#12 mm	#6 mm @ 100 mm c/c
HSC80-FECC-CC-80	200	250	1000	50	100	7	4.2	4-#12 mm	#6 mm @ 80 mm c/c
HSC80-FECC-SF0.6-80	200	250	1000	50	100	7	4.2	4-#12 mm	#6 mm @ 80 mm c/c
HSC80-FECC-1-CC-100	200	250	1000	50	100	7	4.2	6-#12 mm	#6 mm @ 100 mm c/c
HSC80-FECC-1-SF0.6-100	200	250	1000	50	100	7	4.2	6-#12 mm	#6 mm @ 100 mm c/c
HSC80-FECC-1-CC-80	200	250	1000	50	100	7	4.2	6-#12 mm	#6 mm @ 80 mm c/c
HSC80-FECC-1-SF0.6-80	200	250	1000	50	100	7	4.2	6-#12 mm	#6 mm @ 80 mm c/c

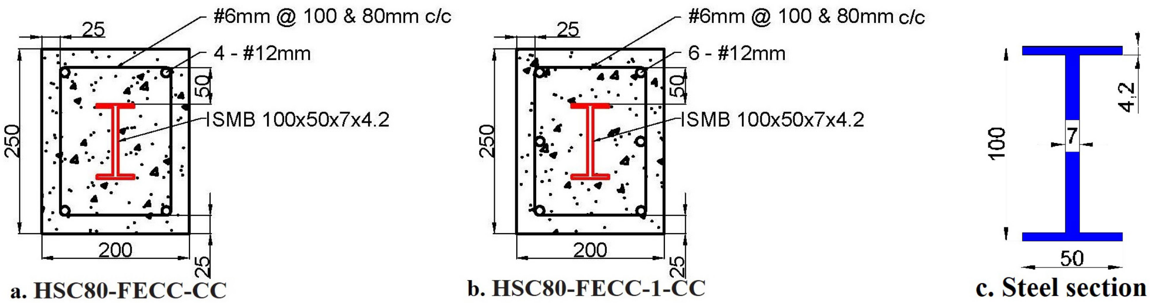

Figure 3: Cross-section details of the column specimens and steel section.

HSC80-FECC-SF0.6-80). The cross-section and longitudinal reinforcement details are illustrated in Figures 3 and 4. For this study, the Indian Standard Medium Beam (ISMB) with dimensions 100 mm × 50 mm × 7 mm × 4.2 mm was used to fabricate the FECC specimens. The steel cage was prepared, and steel sections were placed in the center of the steel cage. The FECC specimens were cast using a steel mould. The steel cage was positioned on the mould, and the high-strength concrete mix was poured and compacted using a vibrator to prevent the formation of honeycomb structures. Finally, the HSC was levelled and left to set for 24 hours at room temperature, as shown in Figure 5. The next day, the specimens were carefully removed from the steel mould without any damage and placed in a water tank for 28 days of curing. After curing, the FECC specimens were removed from the water tank, cleaned on the outer surface, and then whitewashed and marked with specimen numbers for testing.

2.3. Experimental setup and instrumentation

The FECC specimens were placed on the 500 T loading frame and tested until the failure. After placing the specimens, the Linear Variable Differential Transfers (LVDTs) were used; one was placed in the vertical direction, and the remaining two were placed in a vertical direction to measure the vertical and lateral deformation is shown in Figure 6. The specimens are controlled strain, and the loading rate is applied on the specimens at 0.3 mm/minute [4–7, 33, 34]. The boundary condition of the FEC columns used in this study was both end-hinged. Initially, the specimens are tested using 5% of the axial load for accuracy. After that, the values are resent, and the axial load is applied until the FECC specimens are obtained. During the experimental study, the axial load and deformation were recorded in all FECC specimens, and experimental results are discussed in upcoming sections.

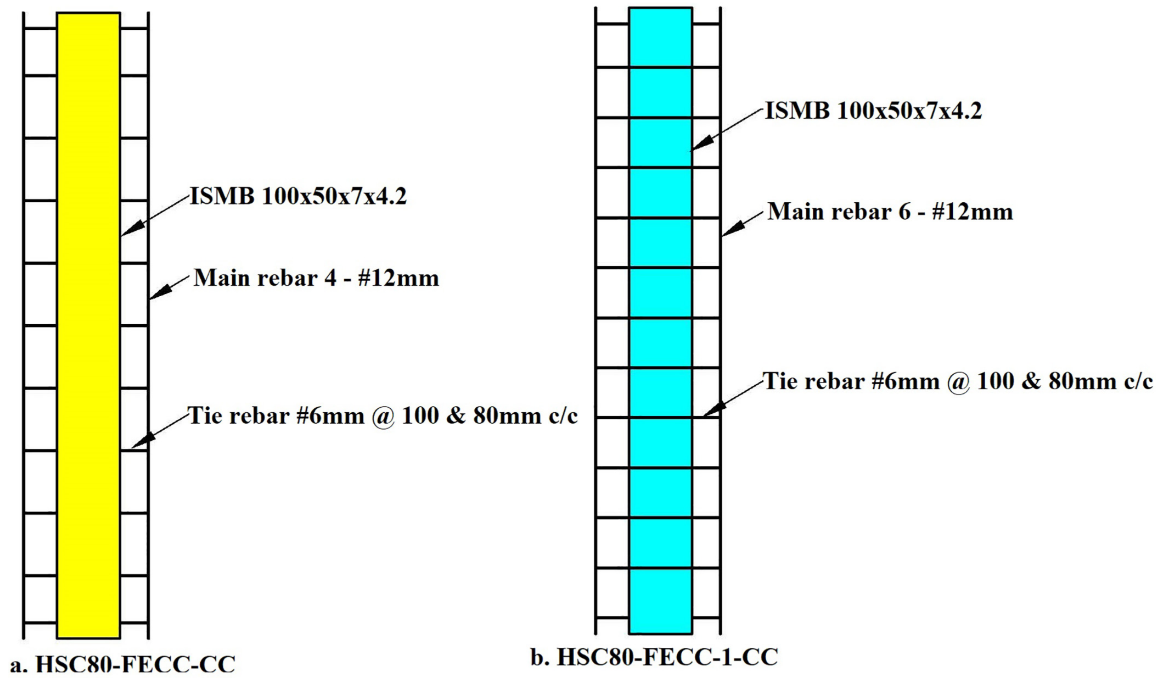

Figure 4: Reinforcement details of FECC specimen.

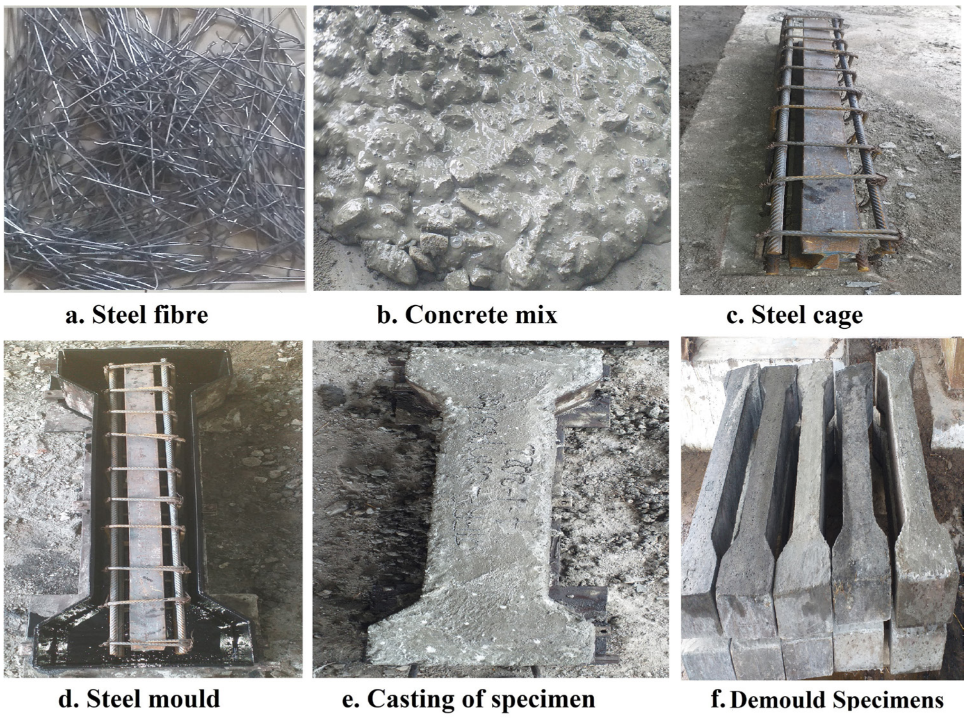

Figure 5: Fabrication of FECC specimens.

3. ANALYTICAL STUDY

In this study, the FECC columns are designed using various codes, like IS: 456 – 2000 [30], JGJ 138 – 2016 [31], and EN-1994-1-1 [32]. The experimental test results are compared to the predicted or analytical results reported in Table 3. The FECC specimens are designed using three equations: (1) to (3). The reduction factors significantly affect the load-carrying capacity of the FECC specimens. Specifically, the IS: 456 – 2000 design codes consider reduction factors of 0.4 for concrete, 0.67 for reinforcement, and 0.87 for steel sections.

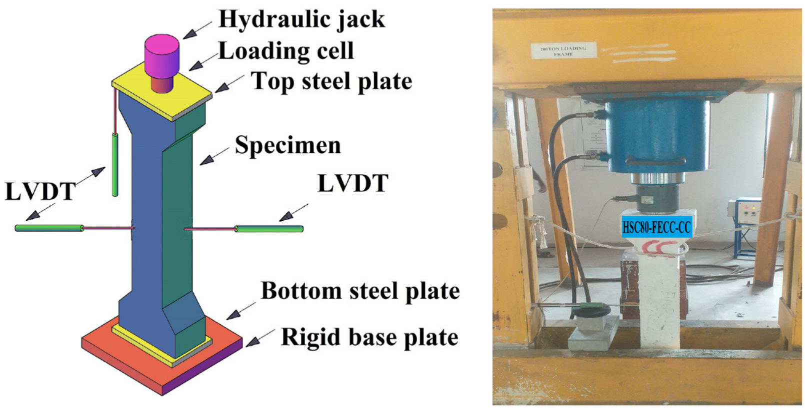

a. 3D model of specimen b.Experimental model

Figure 6: Experimental setup of the specimen.

Table 3: Comparison between experimental and analytical results.

SPECIMEN ID	EXPERIMENTAL LOAD (kN)	ANALYTICAL LOAD (kN)			RATIO		
		IS	JGJ	EC4	P_{Expt}/IS	P_{Expt}/JGJ	P_{Expt}/EC4
HSC80-FECC-CC-100	4024.47	1992.10	4094.54	3895.47	2.02	0.98	1.03
HSC80-FECC-SF0.6-100	4218.64	2127.90	4400.09	4184.04	1.98	0.96	1.01
HSC80-FECC-CC-80	4268.32	1992.10	4094.54	3895.47	2.14	1.04	1.10
HSC80-FECC-SF0.6-80	4453.86	2127.90	4400.09	4184.04	2.09	1.01	1.06
HSC80-FECC-1-CC-100	4198.26	2067.87	4207.64	4008.57	2.03	1.00	1.05
HSC80-FECC-1-SF0.6-100	4368.74	2203.67	4513.19	4297.14	1.98	0.97	1.02
HSC80-FECC-1-CC-80	4456.58	2067.87	4207.64	4008.57	2.16	1.06	1.11
HSC80-FECC-1-SF0.6-80	4647.32	2203.67	4513.19	4297.14	2.11	1.03	1.08
Mean					2.06	1.01	1.06
SD					0.07	0.04	0.04
CV (%)					3.36	3.57	3.54

Similarly, JGJ 138 – 2016 uses a reduction factor 0.9 for concrete, reinforcement, and steel sections. Finally, EN-1994-1-1 employs a reduction factor of 0.85 for concrete.

$$N_{IS} = A_c 0.4 f_{ck} + A_r 0.67 f_{yr} + A_s 0.87 f_{ys} \tag{1}$$

$$N_{JGJ} = 0.9(A_c f_{ck} + A_r f_{yr} + A_s f_{ys}) \tag{2}$$

$$N_{EC4} = 0.85 A_c f_{ck} + A_r f_{yr} + A_s f_{ys} \tag{3}$$

Meanwhile, the letters A_s, A_r, and A_c denote the steel section, longitudinal reinforcing bars, and concrete area. Similarly, f_{yr}, $f_{ys,}$ and f_{ck} represent the longitudinal rebar yield strength, steel section yield strength, and cube compressive strength of concrete.

4. RESULTS AND DISCUSSION

4.1. Axial load versus deformation

The axial load-deformation curves of all FECC specimens are shown in Figure 7. The tested yield, ultimate deformation, and axial load results are reported in Table 4. Based on experimental observations, the FECC specimens (HSC80-FECC-SF0.6-100, HSC80-FECC-1-SF0.6-100, HSC80-FECC-CC-80, HSC80-FECC-SF0.6-80, HSC80-FECC-CC-100, HSC80-FECC-1-SF0.6-100, HSC80-FECC-1-CC-80, and HSC80-FECC-1-SF0.6-80) exhibited linear behaviour up to the yield point [3, 4]. After reaching the yield point, the specimens transitioned from elastic to plastic behaviour [3–7]. Furthermore, the axial load increased until the ultimate load of the specimens reached. Ultimately, the specimens failed after reaching their ultimate load. The axial load carrying capacity improved in all specimens as follows: HSC80-FECC-SF0.6-100: 4024.47 kN, HSC80-FECC-1-SF0.6-100: 4218.64 kN, HSC80-FECC-CC-80: 4268.32 kN, HSC80-FECC-SF0.6-80: 4453.86 kN, HSC80-FECC-CC-100: 4198.26 kN, HSC80-FECC-1-SF0.6-100: 4368.74 kN, HSC80-FECC-1-CC-80: 4456.58 kN, and HSC80-FECC-1-SF0.6-80: 4647.32 kN. These improvements were achieved by adding 0.6% SF and reducing lateral reinforcement spacing.

4.2. Effect of steel fibre on load-carrying capacity of specimens

The steel fibres enhance the axial load-carrying capacity of the FECC specimens, as represented in Figure 8. Additionally, the SF prevent minor cracks and concrete cover spalling [35–40]. The addition of 0.6% steel fibres leads to an improved axial load-carrying capacity of 4.82%, 4.35%, 4.06%, and 4.34% for the following FECC specimens: HSC80-FECC-SF0.6-100, HSC80-FECC-SF0.6-80, HSC80-FECC-1-SF0.6-100, and HSC80-FECC-1-SF0.6-80. These improvements are in comparison to conventional specimens (HSC80-FECC-CC-100, HSC80-FECC-CC-80, HSC80-FECC-1-CC-100, and HSC80-FECC-1-CC-80).

4.3. Ductility and energy absorption of specimen

Ductility is an important factor for RC structures in the design of seismic conditions. Ductility is defined as the ratio between the ultimate and yield deformations of the specimens [41], as shown in Figure 9. Additionally, adding 0.6% SF has improved the ductility of the specimens, as depicted in Figure 10. Specifically, the ductility increased by 12.64%, 7.66%, 3.44%, and 3.79% for the following specimens: HSC80-FECC-SF0.6-100, HSC80-FECC-SF0.6-80, HSC80-FECC-1-SF0.6-100, and HSC80-FECC-1-SF0.6-80. Similarly, for the specimens with reduced lateral reinforcement spacing from 100mm to 80mm, the ductility improved by 11.83%, 6.89%, 7.24%, and 7.59% for the following cases: HSC80-FECC-CC-80, HSC80-FECC-SF0.6-80, HSC80-FECC-1-CC-80, and HSC80-FECC-1-SF0.6-80. The ductility can be calculated using the following equation (4).

$$\text{Ductility index } (\mu_\Delta) = \frac{\Delta u}{\Delta y} \tag{4}$$

The ductility of the FECC specimens was calculated in three stages. In the first stage, the axial load-deformation curve of the specimens is a straight line up to 70% of the axial load, where minor cracks are observed; this stage is denoted as (Δ_y). In the second stage, the axial load is continuously applied to the specimens until the ultimate load is denoted as (Δ_u). During this stage, the specimens may fail partially or entirely, exhibiting wide cracks, concrete cover spalling, fibre pull-out, crushing, and splitting. Similarly, in the third stage, the specimens fail after reaching the ultimate load, denoted as (Δ_f). The ductility increased by adding steel fibres to the concrete mix. These fibres enhance the bond between the cement paste and aggregates, resulting in increased load-carrying capacity of the specimens and reduced deformation. Additionally, steel fibres prevent minor cracks and enhance the load-carrying capacity of the FEC columns [42, 43].

The ultimate energy absorption capacity of all FECC specimens is calculated and presented in Table 5. This capacity is determined by analyzing the yield and ultimate load-deformation curves, as depicted in Figure 11. Notably, the energy absorption capacity is enhanced by adding 0.6% steel fibre. Specifically, the fol-

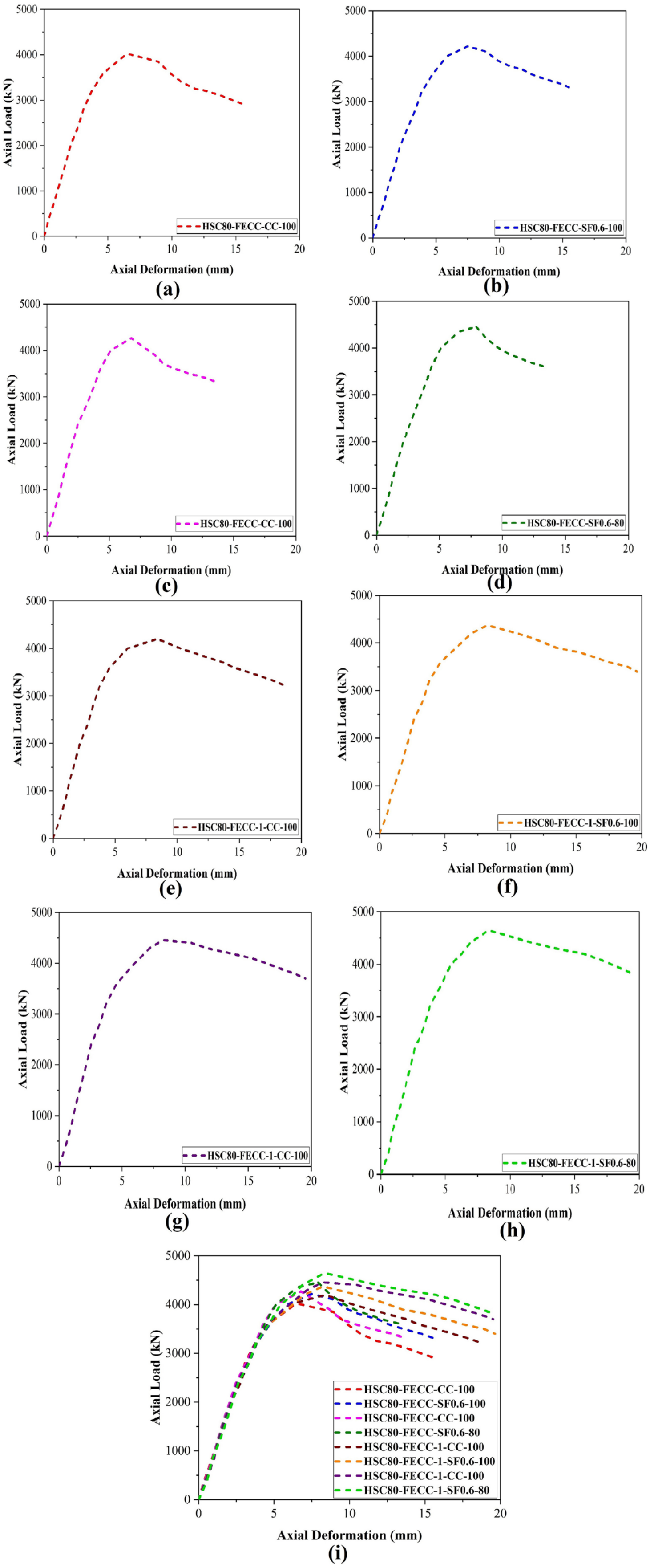

Figure 7: Experimental axial load versus deformation of column specimens. (a) HSC80-FECC-CC-100; (b) HSC80-FECC-SF0.6-100; (c) HSC80-FECC-CC-80; (d) HSC80-FECC-SF0.6-80; (e) HSC80-FECC-1-CC-100; (f) HSC80-FECC--1-SF0.6-100; (g) HSC80-FECC-1-CC-100; (h) HSC80-FECC-1-SF0.6-100; (i) All groups of FECC specimens.

Table 4: Comparison between experimental and analytical results.

SPECIMEN ID	YIELD POINT		ULTIMATE POINT	
	LOAD (kN)	DEFORMATION (mm)	LOAD (kN)	DEFORMATION (mm)
HSC80-FECC-CC-100	2828.13	2.64	4024.47	6.48
HSC80-FECC-SF0.6-100	2933.05	2.72	4218.64	7.52
HSC80-FECC-CC-80	2947.82	2.47	4268.32	6.78
HSC80-FECC-SF0.6-80	3152.70	2.68	4453.86	7.92
HSC80-FECC-1-CC-100	2978.78	2.78	4198.26	8.41
HSC80-FECC-1-SF0.6-100	3087.12	2.63	4368.74	8.23
HSC80-FECC-1-CC-80	3169.61	2.54	4456.58	8.24
HSC80-FECC-1-SF0.6-80	3293.12	2.48	4647.32	8.35

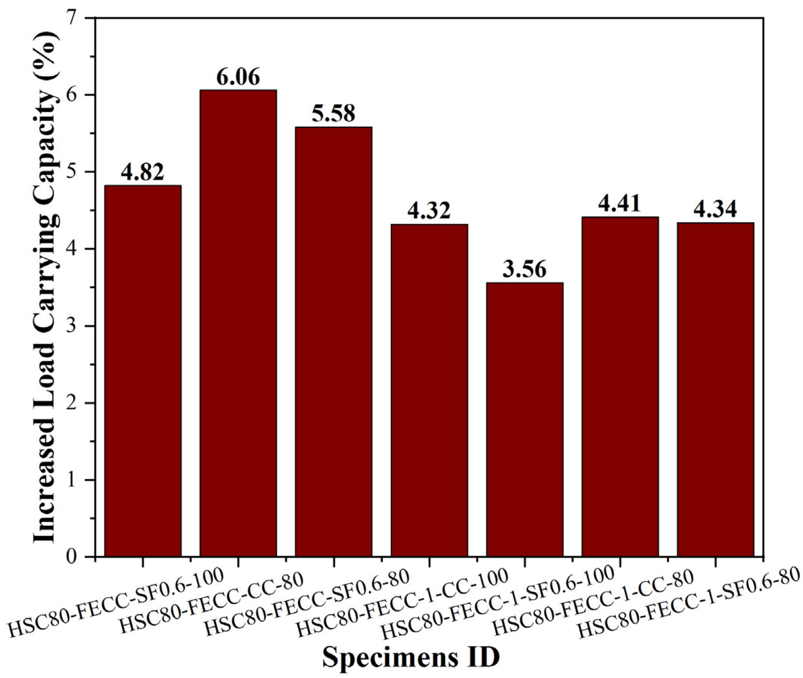

Figure 8: Increased load-carrying capacity of FECC specimens.

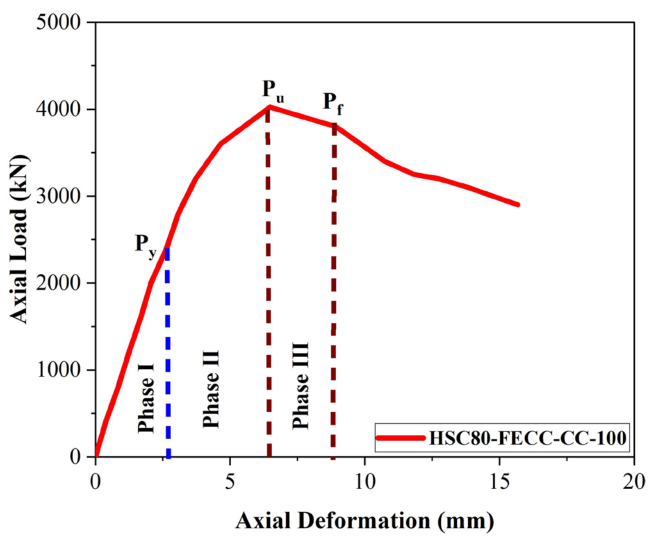

Figure 9: Model of ductility calculation of FECC.

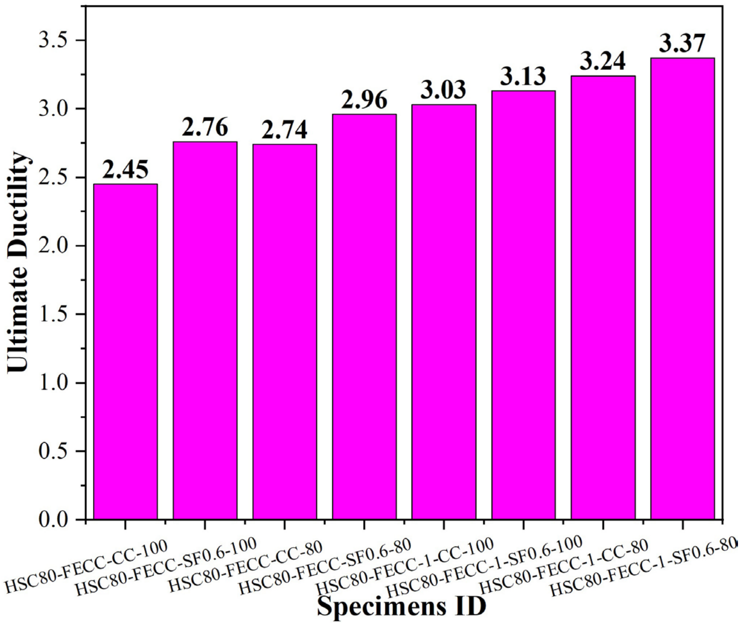

Figure 10: Ultimate ductility of all FECC.

Table 5: Experimental ductility, stiffness, energy absorption and mode of failure of all specimens.

SPECIMEN ID	DUCTILITY	STIFFNESS (kN/mm)	ENERGY ABSORPTION $\times 10^3$ (J)	MODE OF FAILURE
HSC80-FECC-CC-100	2.45	621.06	17.77	CC
HSC80-FECC-SF0.6-100	2.76	560.99	22.12	CC+FP+SP
HSC80-FECC-CC-80	2.74	629.55	21.15	CC+CCS
HSC80-FECC-SF0.6-80	2.96	592.27	25.09	CC+FP
HSC80-FECC-1-CC-100	3.03	499.20	27.18	CC+CCS
HSC80-FECC-1-SF0.6-100	3.13	530.83	28.13	CC+SP
HSC80-FECC-1-CC-80	3.24	540.85	29.21	CC+CCS
HSC80-FECC-1-SF0.6-80	3.37	556.57	31.37	CC+FP+SP

Note: CC - Concrete Crushing; FP - Fibre pull-out; CCS - Concrete Cover Spalling; SP - Splitting.

lowing energy absorption values (in joules) were observed for different specimen types: HSC80-FECC-CC-100: 17.77 J; HSC80-FECC-SF0.6-100: 22.12 J; HSC80-FECC-CC-80: 21.15 J; HSC80-FECC-SF0.6-80: 25.09 J; HSC80-FECC-1-CC-100: 27.18 J; HSC80-FECC-1-SF0.6-100: 28.13 J; HSC80-FECC-1-CC-80: 29.13 J; HSC80-FECC-1-SF0.6-80: 31.27 J. These results are visually presented in Figure 12.

The ultimate stiffness of all FECC specimens is determined and presented in Table 5. Adding steel fibre to the FECC specimens improves the load-carrying capacity while reducing the stiffness of the specimens. In this study, to increase the reinforcement percentages of the FECC specimens (specifically, HSC80-FECC-1-CC-100, HSC80-FECC-1-SF0.6-100, HSC80-FECC-1-CC-80, and HSC80-FECC-1-SF0.6-80), the stiffness of these specimens is intentionally reduced compared to the stiffness of the HSC80-FECC-CC-100, HSC80-FECC-SF0.6-100, HSC80-FECC-CC-80, and HSC80-FECC-SF0.6-80 specimens. This comparison is visually displayed in Figure 13.

4.4. Mode of failure

The failure mode observed from all FECC specimens is reported in Table 5, and failure specimens are shown in Figure 14. The common mode of failure observed from all specimens is concrete crushing. The (HSC80-FECC-CC-100, HSC80-FECC-CC-80, HSC80-FECC-1-CC-100, and HSC80-FECC-1-CC-80) specimen

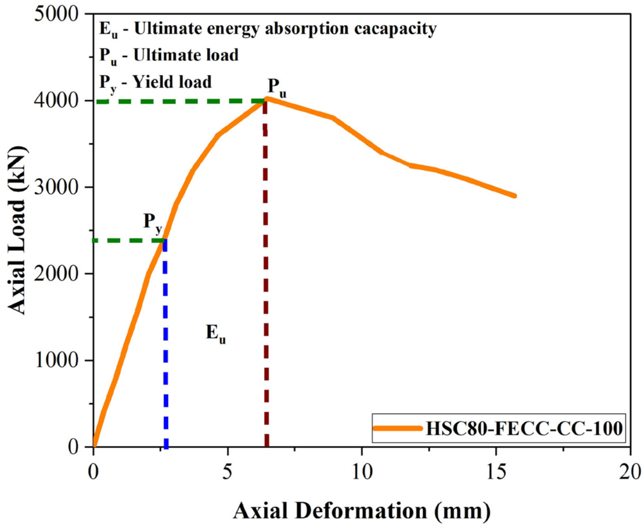

Figure 11: Model of energy absorption calculation of FECCs.

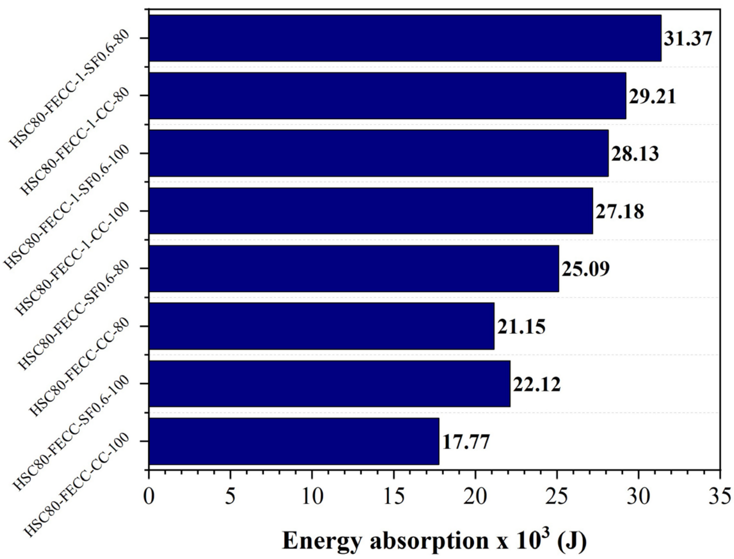

Figure 12: Energy absorption capacity of all FECC.

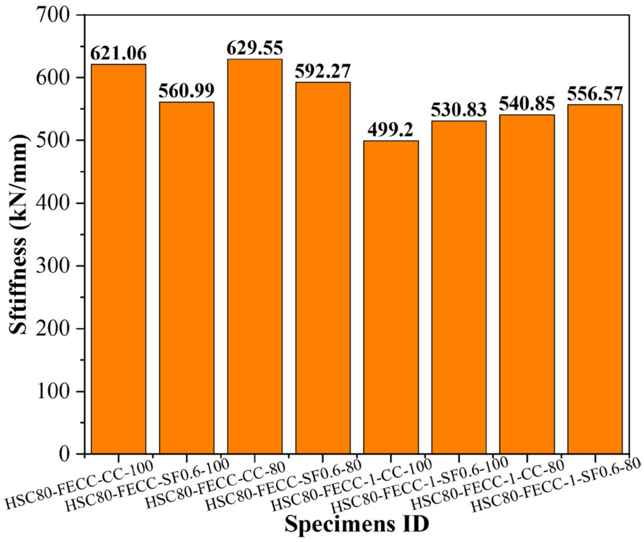

Figure 13: Stiffness of all FECC specimens.

Figure 14: Failed FECC specimens.

failed due to concrete cover spalling and wide cracks, compared to the (HSC80-FECC-SF0.6-100, HSC80-FECC-SF0.6-80, HSC80-FECC-1-SF0.6-100, and HSC80-FECC-1-SF0.6-80) specimens. The addition of 0.6% SF to the concrete mix enhanced the structural performance and, at the same time, prevented concrete cover spalling and cracks [3–7].

The specimens (HSC80-FECC-SF0.6-100, HSC80-FECC-SF0.6-80, HSC80-FECC-1-SF0.6-100, and HSC80-FECC-1-SF0.6-80) failed with minor cracks and fibre pull-out, compared to the (HSC80-FECC-CC-100, HSC80-FECC-CC-80, HSC80-FECC-1-CC-100, and HSC80-FECC-1-CC-80) specimens. Overall observation from the failed specimens indicates that reducing the lateral reinforcement spacing from 100 mm to 80 mm and adding steel fibre to FECC enhances structural performance and prevents cracks and concrete cover spalling [44, 45].

5. STATISTICAL ANALYSIS

The statistical analysis was evaluated using various codes, such as IS: 456 – 2000, JGJ 138 - 2016, and EN-1994-1-1. The experimental test results were compared to the previous literature data [3-10, 20, 46], and the predicted results were highly correlated with the experimental test results, as shown in Table 6. The mean values were 1.57, 0.94, and 0.96, while the standard deviations were 0.43, 0.15, and 0.15 for IS: 456 – 2000, JGJ 138 - 2016, and EN-1994-1-1, respectively. Additionally, the coefficient of variation was 27.19%, 16.36%, and 16.17% for the same codes. The experimental and previously published results were predicted using IS: 456 – 2000, JGJ 138 - 2016, and EN-1994-1-1. Notably, the predicted results from the JGJ 138-2016 and EN-1994-1-1 codes closely aligned with the experimental test results, as depicted in Figure 15. Based on the experimental tests and statistical analysis, the JGJ 138 - 2016 and EN-1994-1-1 codes are highly recommended for predicting the carrying capacity of fully encased composite columns. Furthermore, the graphical representation indicates that the variation between present experimental results and previously published data is only ±15%. The EN-1994-1-1 code introduces two proposed methods: proposed method-1 and proposed method-2. Proposed method one is extended by considering the area of the concrete core. The development of equation (3) leads to equation (5).

$$N_{PM1} = 0.85 A_c f_{ck(core)} + A_r f_{yr} + A_s f_{ys} \tag{5}$$

Similarly, proposed method two is developed using the strength reduction factor (η) [3, 47, 48]. This factor ensures adequate strength prediction for high-strength and ultra-high-strength concrete. By incorporating the strength reduction factor (η) into equation (3) along with two condition factors, we modify it to equation (5).

Conditions: i. $\eta = 1.0$ for $50\ \text{N/mm}^2 < f_c \leq 90\ \text{N/mm}^2$

ii. $\eta = 0.8$ for $f_c > 90\ \text{N/mm}^2$

$$N_{PM2} = 0.85 \eta A_c f_{ck} + A_r f_{yr} + A_s f_{ys} \tag{6}$$

The experimental test results were compared to the proposed methods, and the predicted results are reported in Table 7. The prediction results from the proposed methods closely correlate with the analytical and experimental results, as illustrated in Figure 16. These proposed methods (Methods 1 and 2) predict the axial load-carrying capacity of fully encased composite columns. Specifically, the mean values are 1.08 and 1.06,

Table 6: Geometric details and physical properties from the literature survey.

SPECIMEN ID	B × D	STEEL SECTION	TEST RESULTS (MPa)			EXPT (kN)	VARIOUS CODES (kN)			RATIO = EXPT/ANLY			REF.
			f_c	f_{ys}	f_{yr}		IS	JGJ	EC4	IS	JGJ	EC4	
SRC1	280 × 280	150 × 150 × 7 × 10	29.5	296	350	4220	2821.67	4459.66	4344.02	1.50	0.95	0.97	[3]
SRC2	280 × 280		28.1	296	350	4228	2777.77	4360.88	4250.73	1.52	0.97	0.99	
SRC3	280 × 280		29.8	296	350	4399	2831.08	4480.83	4364.02	1.55	0.98	1.01	
SRC4	280 × 280	2*175 × 90 × 5 × 8	29.8	345	350	4441	3398.57	5301.51	5184.70	1.31	0.84	0.86	
SRC5	280 × 280		29.8	345	350	4519	3398.57	5301.51	5184.70	1.33	0.85	0.87	
SRC6	280 × 280		29.5	345	350	4528	3389.17	5280.35	5164.71	1.34	0.86	0.88	
SRC7	280 × 280	150 × 150 × 7 × 10	28.1	303	350	3788	2114.98	3713.59	3603.44	1.79	1.02	1.05	
SRC8	280 × 280		26.4	303	350	3683	2061.67	3593.64	3490.15	1.79	1.02	1.06	
SRC9	280 × 280		28.1	303	350	3630	2114.98	3713.59	3603.44	1.72	0.98	1.01	
SRC10	280 × 280		29.8	303	350	3893	2168.29	3833.54	3716.73	1.80	1.02	1.05	
C50-S120-SF0	240 × 240	153 × 157.6 × 6.5 × 9.4	52.3	375	550	4475	2434.80	4835.05	4684.42	1.84	0.93	0.96	[4]
C120-S120-SF0	240 × 240		125.6	375	550	5936	4123.64	5914.00	5938.00	1.44	1.00	1.00	
C120-S90-SF0	240 × 240		125.6	375	550	6250	4123.64	5914.00	5938.00	1.52	1.06	1.05	
C120-S60-SF0	240 × 240		125.6	375	550	6889	4123.64	5914.00	5938.00	1.67	1.16	1.16	
C120-S120-SF0.5	240 × 240		126.7	375	550	6907	4148.98	5914.00	5938.00	1.66	1.17	1.16	
C120-S60-SF0.5	240 × 240		126.7	375	550	7521	4148.98	5914.00	5938.00	1.81	1.27	1.27	
HSC1-1	150 × 150	100 × 50 × 7 × 4.2	78.19	247	464	1172	1074.99	2224.05	2136.08	1.09	0.53	0.55	[5]
HSC1-2	150 × 150		78.19	247	464	1165	1074.99	2224.05	2136.08	1.08	0.52	0.55	
HSC1-3	150 × 150		78.19	247	464	1180	1074.99	2224.05	2136.08	1.10	0.53	0.55	
HSC2-1	150 × 150		82.6	247	464	1276	1114.68	2313.35	2220.42	1.14	0.55	0.57	
HSC2-2	150 × 150		82.6	247	464	1264	1114.68	2313.35	2220.42	1.13	0.55	0.57	
HSC2-3	150 × 150		82.6	247	464	1289	1114.68	2313.35	2220.42	1.16	0.56	0.58	
FECC-1	200 × 200	100 × 50 × 7 × 4.2	79	250	500	2034	1651.74	2347.00	2425.00	1.23	0.87	0.84	[6]
FECC-1	200 × 230		79	250	500	2187	1939.73	2387.00	2378.00	1.13	0.92	0.92	
FECC-1	200 × 250		79	250	500	2315	2164.53	2762.00	2835.00	1.07	0.84	0.82	

Continue...

Table 6: *Continued....*

SPECIMEN ID	B × D	STEEL SECTION	TEST RESULTS (MPa)			EXPT (kN)	VARIOUS CODES (kN)			RATIO = EXPT/ANLY			REF.
			f_c	f_{ys}	f_{yr}		IS	JGJ	EC4	IS	JGJ	EC4	
C-100-SF0	200 × 200	100 × 50 × 7 × 4.2	86.42	248.64	546	3624	1787.52	3846.04	3673.20	2.03	0.94	0.99	[7]
C-100-SF0.6	200 × 200		94.76	248.64	546	3963	1920.96	4146.28	3956.76	2.06	0.96	1.00	
C-80-SF0	200 × 200		86.42	248.64	546	3764	1787.52	3846.04	3673.20	2.11	0.98	1.02	
C-80-SF0.6	200 × 200		94.76	248.64	546	4127	1920.96	4146.28	3956.76	2.15	1.00	1.04	
C-60-SF0	200 × 200		86.42	248.64	546	3897	1787.52	3846.04	3673.20	2.18	1.01	1.06	
C-60-SF0.6	200 × 200		94.76	248.64	546	4347	1920.96	4146.28	3956.76	2.26	1.05	1.10	
SRC1	280 × 280	2*175 × 90 × 5 × 8	23.9	274	453	3602	2700.00	3903.20	3809.51	1.33	0.92	0.95	[8]
SRC2	280 × 280		23.5	274	453	3502	1763.39	3874.97	3782.85	1.99	0.90	0.93	
SRC3	280 × 280		21.8	274	453	3836	2400.00	3755.02	3669.56	1.60	1.02	1.05	
SRC4	280 × 280		25.3	271	453	3854	1988.84	4123.22	4024.04	1.94	0.93	0.96	
C1	200 × 200	110	18.48	240	400	1050	950.00	1080.00	1090.00	1.11	0.97	0.96	[9]
C2	200 × 200		18.48	240	400	1170	1353.43	1210.00	1240.00	0.86	0.97	0.94	
CSRC1	400 × 400	170 × 150 × 7 × 10	26.88	301.7	357	5950	2872.55	5682.36	5467.32	2.07	1.05	1.09	[10]
CSRC2	400 × 400		35.2	301.7	357	6664	3405.03	6880.44	6598.84	1.96	0.97	1.01	
CSRC3	400 × 400		35.2	301.7	357	7009	3405.03	6880.44	6598.84	2.06	1.02	1.06	
CSRC4	400 × 400	175 × 175 × 7.5 × 11	26.88	296.7	357	6517	2873.02	5704.61	5489.57	2.27	1.14	1.19	
CSRC5	400 × 400		35.2	296.7	357	6771	3405.50	6902.69	6621.09	1.99	0.98	1.02	
C-1-M40	200 × 200	110	93	253	427	3862	3410.95	3810.00	3825.00	1.13	1.01	1.01	[20]
C-1-M60	200 × 200		93	253	427	3789	3410.95	3810.00	3825.00	1.11	0.99	0.99	
C-1-M80	200 × 200		93	253	427	3809	3410.95	3810.00	3825.00	1.12	1.00	1.00	
C-1-M40	200 × 200	2*100	93	253	427	3838	3410.95	3810.00	3825.00	1.13	1.01	1.00	
C-1-M60	200 × 200		93	253	427	4165	3410.95	3810.00	3825.00	1.22	1.09	1.09	
C-1-M40	200 × 200		94	253	427	4104	3669.35	4206.00	4228.00	1.12	0.98	0.97	
C-1-M60	200 × 200		94	253	427	4180	3669.35	4206.00	4228.00	1.14	0.99	0.99	
C-1-M80	200 × 200		94	253	427	3855	3669.35	4206.00	4228.00	1.05	0.92	0.91	
C-1-M40	200 × 200		94	253	427	4010	3669.35	4206.00	4228.00	1.09	0.95	0.95	

Continue...

Table 6: *Continued....*

SPECIMEN ID	B × D	STEEL SECTION	TEST RESULTS (MPa)			EXPT (kN)	VARIOUS CODES (kN)			RATIO = EXPT/ANLY			REF.
			f_c	f_{ys}	f_{yr}		IS	JGJ	EC4	IS	JGJ	EC4	
C-1-M60	201 × 200		94	253	427	4010	3669.35	4206.00	4228.00	1.09	0.95	0.95	
NS-N1	160 × 160	46 × 80 × 5.2 × 3.8	24	240	360	635	627.21	782.00	796.00	1.01	0.81	0.80	[46]
HS-N1	160 × 160		56	240	360	922	954.89	935.00	918.00	0.97	0.99	1.00	
NS-W1	160 × 160	92 × 80 × 6 × 6	24	240	360	1099	753.58	1300.11	1269.39	1.46	0.85	0.87	
HS-W1	160 × 160		56	240	360	1550	1081.26	2037.39	1965.71	1.43	0.76	0.79	
HSC80-FECC-CC-100	200 × 250	100 × 50 × 7 × 4.2	79.63	246.72	486.42	4024.47	1972.49	4249.48	4050.40	2.04	0.95	0.99	Author
HSC80-FECC-SF0.6-100	200 × 250		86.42	246.72	486.42	4218.64	2108.29	4555.03	4338.98	2.00	0.93	0.97	
HSC80-FECC-CC-80	200 × 250		79.63	246.72	486.42	4268.32	1972.49	4249.48	4050.40	2.16	1.00	1.05	
HSC80-FECC-SF0.6-80	200 × 250		86.42	246.72	486.42	4453.86	2108.29	4555.03	4338.98	2.11	0.98	1.03	
HSC80-FECC-1-CC-100	200 × 250		79.63	246.72	486.42	4198.26	2068.21	4305.29	4106.21	2.03	0.98	1.02	
HSC80-FECC-1-SF0.6-100	200 × 250		86.42	246.72	486.42	4368.74	2204.01	4610.84	4394.79	1.98	0.95	0.99	
HSC80-FECC-1-CC-80	200 × 250		79.63	246.72	486.42	4456.58	2068.21	4305.29	4106.21	2.15	1.04	1.09	
HSC80-FECC-1-SF0.6-80	200 × 250		86.42	246.72	486.42	4647.32	2204.01	4610.84	4394.79	2.11	1.01	1.06	
Mean	–	–	–	–	–	–	–		–	1.57	0.94	0.96	
SD	–	–	–	–	–	–	–		–	0.43	0.15	0.15	
CV (%)	–	–	–	–	–	–	–		–	27.19	16.36	16.17	

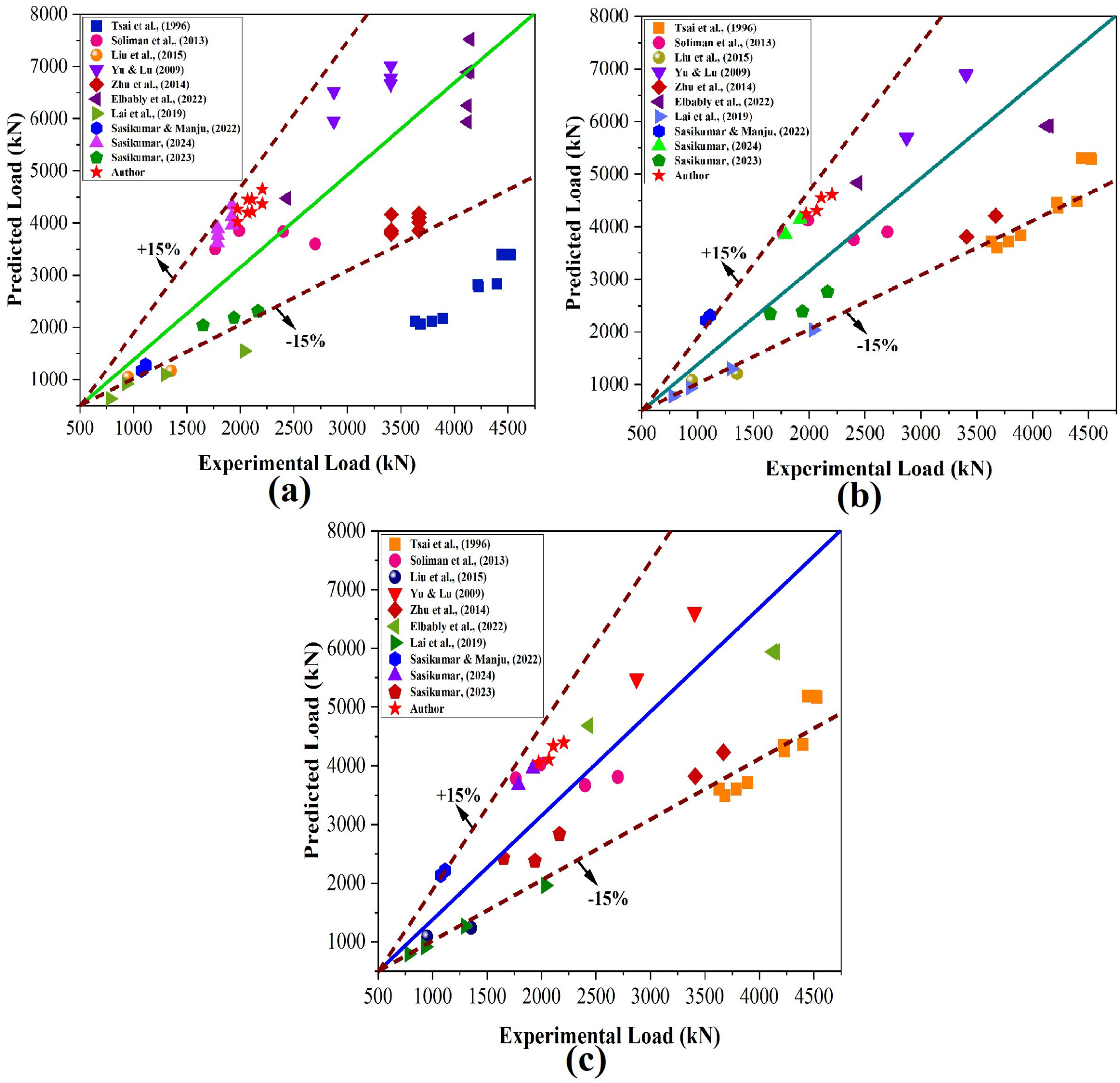

Figure 15: Comparative study between experimental and predicted results from literature studies. (a) IS prediction; (b) JGJ prediction; (c) EC4 prediction.

the standard deviations are 0.04 and 0.04, and the coefficients of variation are 3.54% and 3.53% for proposed methods 1 and 2, respectively. Comparing the reliability of all codes and proposed methods, the graphical representation in Figure 17 supports the recommendation of JGJ 138-2016 and EN-1994-1-1 design codes, along with the proposed methods, for designing the load-carrying capacity of FECCs.

6. CONCLUSIONS

The current research has examined the eight FECCs made with HSC. The specimens are cast with different spacings of tie reinforcement and a 0.6% addition of steel fibre. The experimental tests are compared to the various codes and statistical studies. The following conclusions are based on the experimental, analytical and statistical study.

1. The addition of 0.6% steel fibre enhanced the load-carrying capacity of the FECCs by the following percentages: For HSC80-FECC-SF0.6-100: 4.82%; For HSC80-FECC-SF0.6-80: 4.35%; For HSC80-FECC-1-SF0.6-100: 4.06%; For HSC80-FECC-1-SF0.6-80: 4.28%.These improvements were observed when compared to the control FEC columns without steel fibre: HSC80-FECC-CC-100, HSC80-FECC-CC-80, HSC80-FECC-1-CC-100 and HSC80-FECC-1-CC-80.
2. To reduce the lateral reinforcement spacing of FECCs, the load-carrying capacity of the fully encased columns increased by 6.06%, 5.58%, 6.15%, and 6.38% for HSC80-FECC-CC-80, HSC80-FECC-SF0.6-80,

Table 7: Evaluation of the experimental and analytical results from the proposed methods.

SPECIMEN ID	EXPT LOAD (kN)	ANLY LOAD (kN)			STATISTICAL LOAD (kN)		RATIO = EXPT / ANLY			RATIO = Expt / PRED	
		IS	JGJ	EC4	PM1	PM2	IS	JGJ	EC4	PM1	PM2
HSC80-FECC-CC-100	4024.47	1992.10	4094.54	3895.47	3815.84	3895.47	2.02	0.98	1.03	1.05	1.03
HSC80-FECC-SF0.6-100	4218.64	2127.90	4400.09	4184.04	4097.62	4184.04	1.98	0.96	1.01	1.03	1.01
HSC80-FECC-CC-80	4268.32	1992.10	4094.54	3895.47	3815.84	3895.47	2.14	1.04	1.10	1.12	1.10
HSC80-FECC-SF0.6-80	4453.86	2127.90	4400.09	4184.04	4097.62	4184.04	2.09	1.01	1.06	1.09	1.06
HSC80-FECC-1-CC-100	4198.26	2067.87	4207.64	4008.57	3928.94	4008.57	2.03	1.00	1.05	1.07	1.05
HSC80-FECC-1-SF0.6-100	4368.74	2203.67	4513.19	4297.14	4210.72	4297.14	1.98	0.97	1.02	1.04	1.02
HSC80-FECC-1-CC-80	4456.58	2067.87	4207.64	4008.57	3928.94	4008.57	2.16	1.06	1.11	1.13	1.11
HSC80-FECC-1-SF0.6-80	4647.32	2203.67	4513.19	4297.14	4210.72	4297.14	2.11	1.03	1.08	1.10	1.08
Mean	–		–	–	–	–	2.06	1.01	1.06	1.08	1.06
SD	–		–	–	–	–	0.07	0.04	0.04	0.04	0.04
CV (%)	–		–	–	–	–	3.36	3.57	3.54	3.53	3.54

HSC80-FECC-1-CC-80, and HSC80-FECC-1-SF0.6-80, respectively, compared to HSC80-FECC-CC-100, HSC80-FECC-SF0.6-100, HSC80-FECC-1-CC-100, and HSC80-FECC-1-SF0.6-100.

3. Similarly, the ductility also improved with the addition of 0.6% SF by 12.64%, 7.66%, 3.44%, and 3.79% for HSC80-FECC-SF0.6-100, HSC80-FECC-SF0.6-80, HSC80-FECC-1-SF0.6-100, and HSC80-FECC-1-SF0.6-80, respectively, compared to HSC80-FECC-CC-100, HSC80-FECC-CC-80, HSC80-FECC-1-CC-100, and HSC80-FECC-1-CC-80.
4. Simultaneously, the ductility is enhanced by reducing the tie reinforcement spacing from 100 mm to 80 mm. This reduction results in improvements of 11.83%, 6.89%, 7.24%, and 7.59% for the following cases: HSC80-FECC-CC-80, HSC80-FECC-SF0.6-80, HSC80-FECC-1-CC-80, and HSC80-FECC-1-SF0.6-80, respectively, when compared to their counterparts with 100mm spacing: HSC80-FECC-CC-100, HSC80-FECC-SF0.6-100, HSC80-FECC-1-CC-100, and HSC80-FECC-1-SF0.6-100.
5. The experimental results were compared with various codes, including IS: 456 – 2000, JGJ 138-2016, and EN-1994-1-1. The experimental results aligned well with the analytical predictions for JGJ 138-2016, in contrast to the other two codes. Specifically, the mean, standard deviation, and coefficient variation were as follows: (2.06, 0.07, and 3.36) for IS: 456 – 2000, (1.01, 0.04, and 3.57) for JGJ 138-2016, and (2.06, 0.07, and 3.36) for EN-1994-1-1.
6. Additionally, including 0.6% steel fibre and reduced tie reinforcement significantly enhanced the structural performance of the FECC specimens. The addition of 0.6% SF prevented concrete cover spalling and cracking. The FECC specimens (HSC80-FECC-SF0.6-100, HSC80-FECC-SF0.6-80, HSC80-FECC-1-SF0.6-100, and HSC80-FECC-1-SF0.6-80) containing 0.6% steel fibre exhibited minor cracks without concrete spalling. Conversely, specimens without steel fibre experienced concrete cover spalling and wide cracks, specifically HSC80-FECC-CC-100, HSC80-FECC-CC-80, HSC80-FECC-1-CC-100, and HSC80-FECC-1-CC-80.
7. The statistical analysis explored two proposed methods for predicting the load-carrying capacity of the specimens. Both proposed methods strongly correlated with the experimental test results and effectively predicted the experimental outcomes. These methods align well with the experimental data and the JGJ 138-2016 code. Specifically, for proposed method 1, the mean, standard deviation, and coefficient variation were 1.08, 0.04, and 3.53%, respectively. For proposed method 2, these values were 1.06, 0.04, and 3.54%.

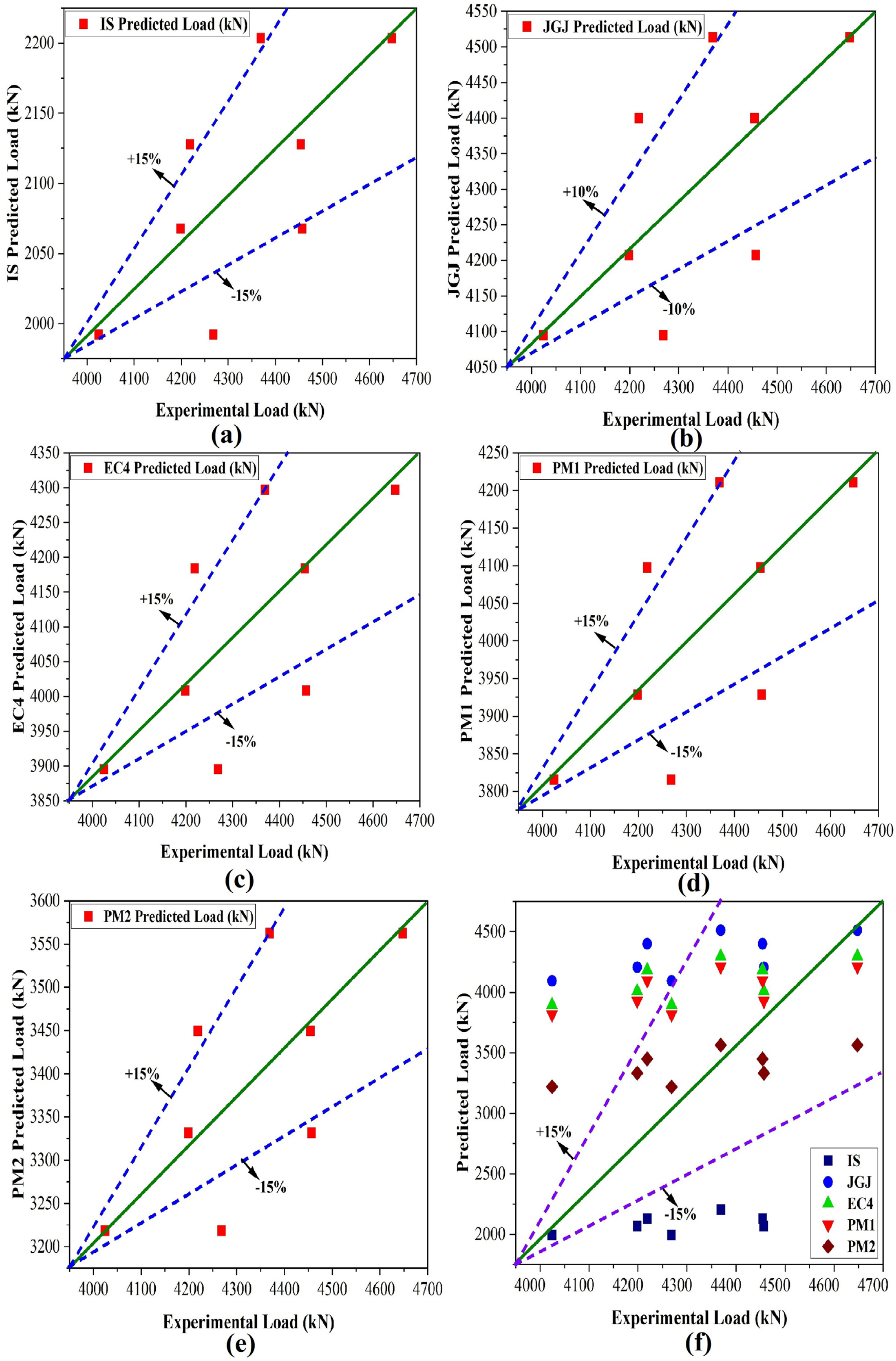

Figure 16: Comparison between experimental and predicted results for various codes and proposed methods. (a) IS prediction; (b) JGJ prediction; (c) EC4 prediction; (d) PM1 prediction; (e) PM2 prediction; (f) overall prediction.

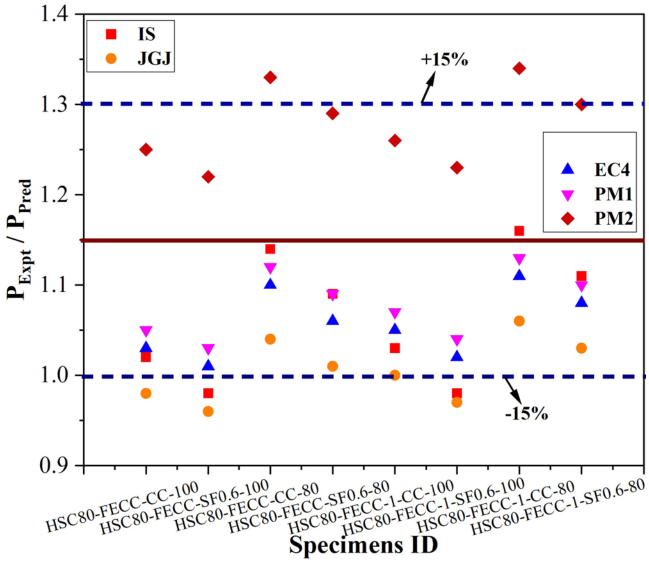

Figure 17: Reliability of experimental and analytical results of FECC specimens.

The research work can be extended to explore various aspects, including different cross-sections, steel sections, fibre content, and concrete grades under varying loading conditions.

7. ACKNOWLEDGMENTS

The authors gratefully acknowledge the Kumaraguru College of Technology and Vivekanandha College of Technology for Women for providing all the required facilities to accomplish this study.

8. BIBLIOGRAPHY

[1] ZHU, M., LIU, J., WANG, Q., *et al.*, “Experimental research on square steel tubular columns filled with steel-reinforced self-consolidating high-strength concrete under axial load”, *Engineering Structures*, v. 32, n. 8, pp. 2278–2286, 2010. doi: http://doi.org/10.1016/j.engstruct.2010.04.002.

[2] CHEN, C.C., YEH, S.C. “Ultimate strength of concrete encased steel composite columns”, *In Proceedings of the third national conference on structural engineering*, pp. 2197–206.

[3] TSAI, K.C., LIEN, Y., CHEN, C.C., “Behaviour of axially loaded steel reinforced concrete columns”, *Journal of the Chinese Institute of Civil and Hydraulic Engineering*, v. 8, n. 4, pp. 535–545, 1996.

[4] LAI, B., LIEW, J.R., XIONG, M., “Experimental study on high strength concrete encased steel composite short columns”, *Construction & Building Materials*, v. 228, pp. 116640, 2019. doi: http://doi.org/10.1016/j.conbuildmat.2019.08.021.

[5] SASIKUMAR, P., MANJU, R., “Performance of high strength concrete encased steel composite columns”, *Revista Română de Materiale*, v. 52, n. 4, pp. 374–384, 2022.

[6] SASIKUMAR, P., “A comparative study between buckling behaviour and statistical analysis of axially loaded fully encased composite columns made with high strength concrete”, *Revista de la Construcción*, v. 22, n. 3, pp. 694–706, 2023. doi: http://doi.org/10.7764/RDLC.22.3.694.

[7] SASIKUMAR, P., “Experimental study on the fully encased composite short columns made with high-strength fibre-reinforced concrete”, *Asian Journal of Civil Engineering*, v. 25, n. 4, pp. 3239, 2024. doi: http://doi.org/10.1007/s42107-023-00975-w.

[8] SOLIMAN, K.Z., ARAFA, A.I., ELRAKIB, T.M., “Review of design codes of concrete encased steel short columns under axial compression”, *HBRC Journal*, v. 9, n. 2, pp. 134–143, 2013.

[9] LIU, Y., GUO, Z.X., XU, P.H., *et al.*, “Experimental study on axial compression behavior of core steel reinforced concrete columns”, *Journal of Building Structures*, v. 36, n. 4, pp. 68–74, 2015.

[10] YU, Q., LU, Z.D., “Research on the static performance of eccentric steel reinforced concrete column”, *Building Structure*, v. 39, n. 6, pp. 34–38, 2009.

[11] TOKGOZ, S., DUNDAR, C., “Experimental tests on biaxially loaded concrete-encased composite columns”, *Steel and Composite Structures*, v. 8, n. 5, pp. 423–438, 2008. doi: http://doi.org/10.12989/scs.2008.8.5.423.

[12] DUNDAR, C., TOKGOZ, S., TANRIKULU, A.K., *et al*., "Behaviour of reinforced and concrete-encased composite columns subjected to biaxial bending and axial load", *Building and Environment*, v. 43, n. 6, pp. 1109–1120, 2008. doi: http://doi.org/10.1016/j.buildenv.2007.02.010.

[13] CAMPIAN, C., NAGY, Z., POP, M., "Behavior of fully encased steel-concrete composite columns subjected to monotonic and cyclic loading", *Procedia Engineering*, v. 117, pp. 439–451, 2015. doi: http://doi.org/10.1016/j.proeng.2015.08.193.

[14] ELLOBODY, E., YOUNG, B., "Numerical simulation of concrete encased steel composite columns", *Journal of Constructional Steel Research*, v. 67, n. 2, pp. 211–222, 2011. doi: http://doi.org/10.1016/j.jcsr.2010.08.003.

[15] LE HOANG, A., FEHLING, E., "Influence of steel fiber content and aspect ratio on the uniaxial tensile and compressive behavior of ultra-high performance concrete", *Construction & Building Materials*, v. 153, pp. 790–806, 2017. doi: http://doi.org/10.1016/j.conbuildmat.2017.07.130.

[16] ZHU, W.Q., MENG, G., JIA, J.Q. "Experimental studies on axial load performance of high-strength concrete short columns"*, Proceedings of the Institution of Civil Engineers-Structures and Buildings*, v. 167, n. 9, pp. 509–519, 2014. doi: http://doi.org/10.1680/stbu.13.00027.

[17] KIM, C.S., PARK, H.G., CHUNG, K.S., *et al*., "Eccentric axial load testing for concrete-encased steel columns using 800 MPa steel and 100 MPa concrete", *Journal of Structural Engineering*, v. 138, n. 8, pp. 1019–1031, Aug. 2012. doi: http://doi.org/10.1061/(ASCE)ST.1943-541X.0000533.

[18] KIM, C.S., PARK, H.G., CHUNG, K.S., *et al*., "Eccentric axial load capacity of high-strength steel-concrete composite columns of various sectional shapes", *Journal of Structural Engineering*, v. 140, n. 4, pp. 04013091, Apr. 2014. doi: http://doi.org/10.1061/(ASCE)ST.1943-541X.0000879.

[19] LAI, B., LIEW, J.R., WANG, T., "Buckling behaviour of high strength concrete encased steel composite columns", *Journal of Constructional Steel Research*, v. 154, pp. 27–42, 2019. doi: http://doi.org/10.1016/j.jcsr.2018.11.023.

[20] ZHU, W., JIA, J., GAO, J., *et al*., "Experimental study on steel reinforced high-strength concrete columns under cyclic lateral force and constant axial load", *Engineering Structures*, v. 125, pp. 191–204, 2016. doi: http://doi.org/10.1016/j.engstruct.2016.07.018.

[21] AMERICAN INSTITUTE OF STEEL CONSTRUCTION, *Manual of Steel Construction. Load & Resistance Factor Design*, 2nd ed., Chicago, IL, AISC, 1994.

[22] PACHIDEH, G., GHOLHAKI, M., MOSHTAGH, A., "An experimental study on cyclic performance of the geometrically prismatic concrete-filled double skin steel tubular (CFDST) columns", *Civil Engineering (Shiraz)*, v. 45, n. 2, pp. 629–638, Jun. 2021. doi: http://doi.org/10.1007/s40996-020-00410-z.

[23] PACHIDEH, G., GHOLHAKI, M., MOSHTAGH, A., "Impact of temperature rise on the seismic performance of concrete-filled double skin steel columns with prismatic geometry", *Journal of Testing and Evaluation*, v. 49, n. 4, pp. 2800–2815, 2021. doi: http://doi.org/10.1520/JTE20200037.

[24] PACHIDEH, G., GHOLHAKI, M., "An experimental study on the effects of adding steel and polypropylene fibers to concrete on its resistance after different temperatures", *Journal of Testing and Evaluation*, v. 47, n. 2, pp. 1606–1620, 2019. doi: http://doi.org/10.1520/JTE20170145.

[25] GHOLHAKI, M., PACHIDEH, G., REZAYFAR, O., "An experimental study on mechanical properties of concrete containing steel and polypropylene fibers at high temperatures", *Journal of Structural and Construction Engineering*, v. 4, n. 3, pp. 167–179, 2017.

[26] BEGUM, M., DRIVER, R.G., ELWI, A.E., "Finite-element modeling of partially encased composite columns using the dynamic explicit method", *Journal of Structural Engineering*, v. 133, n. 3, pp. 326–334, 2007. doi: http://doi.org/10.1061/(ASCE)0733-9445(2007)133:3(326).

[27] CHANG, Q., ZHAO, C., XING, L., *et al*., "Concrete filled double steel tube columns incorporating UPVC pipes under uniaxial compressive load at ambient and elevated temperature", *Case Studies in Construction Materials*, v. 16, pp. e00907, 2022. doi: http://doi.org/10.1016/j.cscm.2022.e00907.

[28] AMIN, A.M.M., FADEL, A.M., GAAWAN, S.M., *et al*., "Assessment the limit of steel core area in the encased composite column", *International Journal of Engineering Research and Applications*, v. 6, n. 3, pp. 72–78, 2016.

[29] ZENG, L., XIAO, Y., CHEN, Y., *et al*., "Seismic damage evaluation of concrete-encased steel frame-reinforced concrete core tube buildings based on dynamic characteristics", *Applied Sciences (Basel, Switzerland)*, v. 7, n. 4, pp. 314, Mar. 2017. doi: http://doi.org/10.3390/app7040314.

[30] BUREAU OF INDIAN STANDARDS, *IS 456 -2000: Plain Concrete and Reinforced*, New Delhi, India, IS, 2000.

[31] REPUBLIC OF CHINA, *JGJ 138-2016: Code for design of composite structures*, China, Ministry of Housing and Urban-Rural Development of the People's Republic of China, 2016.

[32] EUROPEAN COMMITTEE FOR STANDARDIZATION, *EN 1994-1-1: Eurocode 4: Design of composite steel and concrete structures - Part 1.1: General rules and rules for buildings*.

[33] SASIKUMAR, P., MANJU, R., "Structural behaviour of high strength concrete columns reinforced with glass fibre reinforced polymer bars under axial loading", *Revista Romana de Materiale*, v. 52, n .4, pp. 412–423, 2022.

[34] SASIKUMAR, P., MANJU, R., "Structural behavior of axially loaded high strength concrete columns reinforced longitudinally with glass fiber reinforced polymer bars", *Revista de la Construcción*, v. 22, n. 2, pp. 293–305, 2023. doi: http://doi.org/10.7764/RDLC.22.2.293.

[35] ABADEL, A., ABBAS, H., ALMUSALLAM, T., *et al*., "Mechanical properties of hybrid fibre-reinforced concrete-analytical modelling and experimental behaviour", *Magazine of Concrete Research*, v. 68, n. 16, pp. 823–843, 2016.

[36] BISWAS, R.K., BIN AHMED, F., HAQUE, M.E., *et al*., "Effects of steel fiber percentage and aspect ratios on fresh and harden properties of ultra-high performance fiber reinforced concrete", *Applied Mechanics*, v. 2, n. 3, pp. 501–515, 2021. doi: http://doi.org/10.3390/applmech2030028.

[37] WANG, Z., LI, H., ZHANG, X., *et al*., "The effects of steel fiber types and volume fraction on the physical and mechanical properties of concrete", *Coatings*, v. 13, n. 6, pp. 978, May. 2023. doi: http://doi.org/10.3390/coatings13060978.

[38] ZHANG, L., ZHAO, J., FAN, C., *et al*., "Effect of surface shape and content of steel fiber on mechanical properties of concrete", *Advances in Civil Engineering*, v. 1, pp. 8834507, 2020. doi: http://doi.org/10.1155/2020/8834507.

[39] PANI, A.K., SAHOO, K.K., "Study on mechanical properties of steel fibre concrete", In *Recent Developments in Sustainable Infrastructure: Select Proceedings of ICRDSI 2019*, pp. 499–505, 2019.

[40] JANG, S.J., KANG, D.H., AHN, K.L., *et al*., "Feasibility of using high-performance steel fibre reinforced concrete for simplifying reinforcement details of critical members", *International Journal of Polymer Science*, v. 2015, pp. 1–12, 2015. doi: http://doi.org/10.1155/2015/850562.

[41] SASIKUMAR, P., MANJU, R., "Flexural behaviour of reinforced concrete beams reinforced with Glass Fibre Rein-forced Polymer (GFRP) bars: experimental and analytical study", *Asian Journal of Civil Engineering*, v. 25, n. 2, pp. 1–14, 2024.

[42] GEORGE, C., SELVAN, S.S., "Integrated analysis of light gauge steel beam sections enhanced by steel fiber reinforced concrete: a comprehensive study on structural and thermal performance", *Matéria (Rio de Janeiro)*, v. 29, n. 2, pp. e20230329, 2024. doi: http://doi.org/10.1590/1517-7076-rmat-2023-0329.

[43] SASIKUMAR, P., MANJU, R., "Flexural behaviour and strengthening of reinforced concrete beams using concrete canvas", *Asian Journal of Civil Engineering*, v. 25, n. 4, pp. 1–14, 2024. doi: http://doi.org/10.1007/s42107-024-01083-z.

[44] SHAH, S.I., GANESH, G.M., "Micro-steel fiber-reinforced self-compacting concrete-filled steel-tube columns subjected to axial compression", *International Journal of Steel Structures*, v. 23, n. 4, pp. 1031–1045, Aug. 2023. doi: http://doi.org/10.1007/s13296-023-00747-x.

[45] LUNDGREN, K., ROBUSCHI, S., ZANDI, K., "Methodology for testing rebar-concrete bond in specimens from decommissioned structures", *International Journal of Concrete Structures and Materials*, v. 13, n. 1, pp. 38, Dec. 2019. doi: http://doi.org/10.1186/s40069-019-0350-3.

[46] LIEW, J.R., "Design guide for concrete filled tubular members with high strength materials to Eurocode 4", *Research Publishing.* doi: http://doi.org/10.3850/978-981-09-3267-1.

[47] LIEW, J.R., XIONG, M., XIONG, D., "Design of concrete filled tubular beam-columns with high strength steel and concrete", *Structures*, v. 8, pp. 213–226, 2016. doi: http://doi.org/10.1016/j.istruc.2016.05.005.

[48] ELBABLY, A., RAMADAN, O., AKL, A., *et al*., "Behavior of encased steel-high strength concrete columns against axial and cyclic loading", *Journal of Constructional Steel Research*, v. 191, pp. 107161, 2022. doi: http://doi.org/10.1016/j.jcsr.2022.107161.